

Performance Analyses of Noise-Robust Normalized Subband Adaptive Filter Algorithm

Yi Yu^a, Haiquan Zhao^b, Badong Chen^c, Wenyuan Wang^b, Lu Lu^d

Abstract: This paper studies the statistical models of the noise-robust normalized subband adaptive filter (NR-NSAF) algorithm in the mean and mean square deviation senses involving transient-state and steady-state behavior by resorting to the method of the vectorization operation and the Kronecker product. The analysis method does not require the Gaussian input signal. Moreover, the proposed analysis removes the paraunitary assumption imposed on the analysis filter banks as in the existing analyses of subband adaptive algorithms. Simulation results in various conditions demonstrate the effectiveness of our theoretical analysis. For a special form of the algorithm, the proposed steady-state expression is also better accurate than the previous analysis.

Keywords: Noise-robust normalized subband adaptive filter, transient-state and steady-state analyses, correlated input.

1. Introduction

Adaptive filter algorithms have a pivotal position in some applications such as system identification, channel equalization, and echo cancellation [1], [2]. The normalized least mean square (NLMS) algorithm is well-known, owing to its simplicity and ease to implement. Nevertheless, the problem is very slow convergence rate for the correlated input signal. To overcome this problem, subband adaptive filter (SAF) with multiband structure has attracted much attention due to its decorrelation property. The multiband structure eliminates aliasing and band edge effects relative to the conventional structure [3]. Based on this, Lee and Gan introduced the normalized SAF (NSAF) algorithm [3]. Compared with the NLMS, the NSAF obtains faster convergence rate for correlated input signals, while retaining comparable computational complexity. In a recent decade, many works have been reported to further obtain an improvement on the performance of the NSAF [4]-[11]. Typically, inspired by the NLMS with reusing weight vectors at each update [12], a noise-robust NSAF (NR-NSAF) algorithm was proposed which improves the steady-state performance in highly noisy environments [8], and almost at the same time, Ni proposed an improved NSAF (INSAF) algorithm [9].

The performance analysis is very important in studying adaptive algorithms [2], [13]-[17]. Much literature has researched the performance of the NSAF algorithm [18]-[23]. Specifically, the steady-state mean-square error (MSE) of the NSAF using a fixed step size and a regularization constant were studied in [18] and [19], respectively. In some applications such as system identification and echo cancellation, the essence of adaptive filter is to estimate the impulse response of the underlying system, so studying the mean square deviation (MSD) of adaptive algorithms seems to be more appropriate than the MSE. In general, according to their definitions, the MSE can be obtained from the MSD by adding to the covariance matrix of the input vector. In [24], Jeong *et al.* analyzed the steady-state MSD of the INSAF algorithm; and then, such analysis were extended to its under-modeling case [25] and affine projection variant [10]. The theoretical results coincides with the simulations, but the accuracy depends on large number of subbands and long

a School of Information Engineering, Southwest University of Science and Technology, Mianyang, China. (e-mail: yuyi_xyuan@163.com)

b School of Electrical Engineering, Southwest Jiaotong University, Chengdu, China. (e-mail: hqzhao_swjtu@126.com)

c School of Electronic and Information Engineering, Xi'an Jiaotong University, Xi'an, China. (chenbd@mail.xjtu.edu.cn)

d School of Electronics and Information Engineering, Sichuan University, Chengdu, China. (lulu19900303@126.com).

adaptive filter. However, the transient behavior of the INSAF algorithm has not been studied. In this paper, we focus on studying the MSD behavior of the NR-NSAF algorithm as a more general form of the INSAF algorithm. Our analysis is based on the method of the vectorization operation and the Kronecker product developed originally by Sayed [2]. This method is very popular recently, since it does not restrict the input signal to being a specified model (e.g., Gaussian distribution). The contributions of the paper are summarized as follows: 1) analyzing the transient-state and steady-state MSD of the NR-NSAF algorithm; 2) providing the mean condition on the step-size to ensure the algorithm stability. Moreover, the proposed analysis does not require the paraunitary assumption on the analysis filter banks which was extensively used in the analysis of subband adaptive algorithms. Extensive simulations verify the proposed theoretical results.

Notations: $(\cdot)^T$ denotes the transpose of a matrix or vector; $\|\cdot\|_2$ denotes the Euclidean norm of a vector; $E\{\cdot\}$ is to take the expectation of random variables; $\lambda_{\max}(\cdot)$ is the largest eigenvalue of a matrix; $\text{Tr}(\cdot)$ is the trace of a matrix; $\rho(\cdot)$ is the spectral radius of its matrix argument. We use $\text{diag}\{\cdot\}$ to denote the diagonal matrix consisting of diagonal entries and \otimes to denote the Kronecker product. The notation $\text{vec}(\cdot)$ replaces an $M \times M$ matrix by an $M^2 \times 1$ column vector whose entries are formed by stacking the successive columns of the matrix on top of each other, and $\text{vec}^{-1}(\cdot)$ is the inverse operation of $\text{vec}(\cdot)$. The symbols \mathbf{I} and $\mathbf{0}$ denote the identity matrix and zero matrix of appropriate sizes, respectively. In addition, all vectors are column vectors.

2. The NR-NSAF Algorithm

Consider the desired signal $d(n)$ that originates from the model

$$d(n) = \mathbf{u}^T(n) \mathbf{w}_o + \eta(n), \quad (1)$$

where \mathbf{w}_o is an M -length column vector to be estimated, $\mathbf{u}(n) = [u(n), u(n-1), \dots, u(n-M+1)]^T$ is the input vector. The system noise $\eta(n)$ is independent of $u(n)$. Fig. 1 shows the multiband-structured SAF, where N denotes the number of subbands. The input signal $u(n)$ and the desired signal $d(n)$ are partitioned into multiple subband signals $u_i(n)$ and $d_i(n)$ by the analysis filters $H_i(z)$, $i = 0, 1, \dots, N-1$, respectively. The subband outputs $y_i(n)$ are obtained by filtering signals $u_i(n)$ through a fullband adaptive filter whose weight vector denoted as $\mathbf{w}(k) = [w_1(k), w_2(k), \dots, w_M(k)]^T$. Then, signals $y_i(n)$ and $d_i(n)$ are N -fold decimated to yield signals $y_{i,D}(k)$ and $d_{i,D}(k)$ with a lower sampling rate, respectively. We here use n to represent the original sequences and k to represent the decimated sequences. The decimated error signal at the i -th subband is expressed as

$$e_{i,D} = d_{i,D}(k) - \mathbf{u}_i^T(k) \mathbf{w}(k), \quad (2)$$

where $\mathbf{u}_i(k) = [u_i(kN), u_i(kN-1), \dots, u_i(kN-M+1)]^T$ and $d_{i,D}(k) = d_i(kN)$.

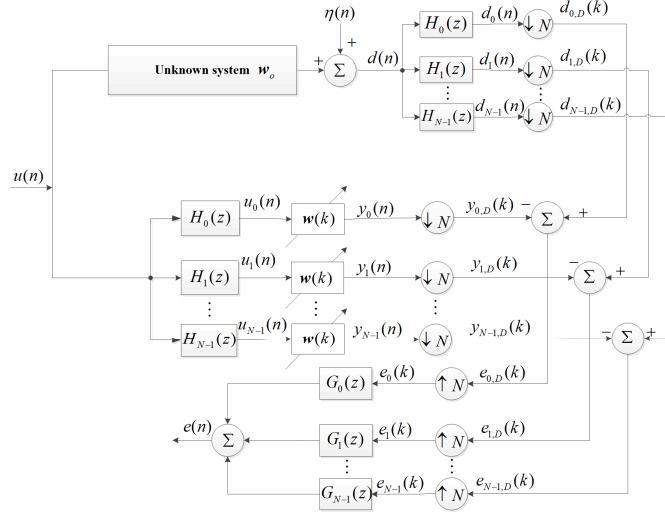


Fig. 1 Multiband structure of SAF.

In [8], the weight vector update of the NR-NSAF algorithm is described as

$$\mathbf{w}(k+1) = \sum_{p=0}^{P-1} \beta_p \mathbf{w}(k-p) + \mu \sum_{i=0}^{N-1} \frac{\zeta_{i,D}(k) \mathbf{u}_i(k)}{\|\mathbf{u}_i(k)\|_2^2 + \varepsilon}, \quad (3)$$

$$\zeta_{i,D} = d_{i,D}(k) - \mathbf{u}_i^T(k) \sum_{p=0}^{P-1} \beta_p \mathbf{w}(k-p), \quad (4)$$

where $\beta_p = \left(\sum_{p=0}^{P-1} \alpha^p\right)^{-1} \alpha^p$, α ($0 < \alpha \leq 1$) is a weighting factor, $\mu > 0$ is the step-size, $\varepsilon > 0$ is a small regularization constant to avoid division by zero, and P denotes the number of reusing past weight vectors at each iteration. The appendix in [11] has given that $0 < \mu < 2$ can guarantee the mean square convergence of the NR-NSAF algorithm. Note that, the NR-NSAF algorithm becomes the INSFAF algorithm when $\alpha = 1$, and reduces to the NSAF algorithm when $P = 1$ or $\alpha = 0$.

3. Performance analyses

Before proceeding, we introduce matrices: $\mathbf{U}(k) = [\mathbf{u}(kN), \mathbf{u}(kN-1), \dots, \mathbf{u}(kN-L+1)]$, $\mathbf{H} = [\mathbf{h}_0, \mathbf{h}_1, \dots, \mathbf{h}_{N-1}]$, and vectors: $\mathbf{d}(k) = [d(kN), d(kN-1), \dots, d(kN-L+1)]^T$, $\mathbf{u}(kN) = [u(kN), u(kN-1), \dots, u(kN-M+1)]^T$, where \mathbf{h}_i , $i = 0, \dots, N-1$ are the impulse responses of the analysis filters with length of L . Thus, we have

$$\mathbf{U}_D(k) \triangleq [\mathbf{u}_0(k), \mathbf{u}_1(k), \dots, \mathbf{u}_{N-1}(k)] = \mathbf{U}(k) \mathbf{H}, \quad (5)$$

$$\mathbf{d}_D(k) \triangleq [d_{0,D}(k), d_{1,D}(k), \dots, d_{N-1,D}(k)]^T = \mathbf{H}^T \mathbf{d}(k), \quad (6)$$

$$\mathbf{d}(k) = \mathbf{U}^T(k) \mathbf{w}_o + \boldsymbol{\eta}(k), \quad (7)$$

where $\boldsymbol{\eta}(k) = [\eta(kN), \eta(kN-1), \dots, \eta(kN-L+1)]^T$. According to (5) and (6), we are able to combine (3) and (4) as:

$$\mathbf{w}(k+1) = \sum_{p=0}^{P-1} \beta_p \mathbf{w}(k-p) + \mu \mathbf{U}(k) \mathbf{H} \mathbf{A}^{-1}(k) \left[\mathbf{H}^T \mathbf{d}(k) - \mathbf{H}^T \mathbf{U}^T(k) \sum_{p=0}^{P-1} \beta_p \mathbf{w}(k-p) \right], \quad (8)$$

where $\mathbf{A}(k) = \varepsilon \mathbf{I}_N + \text{diag}\{\mathbf{U}_D^T(k)\mathbf{U}_D(k)\}$.

Defining the weight error vector as $\tilde{\mathbf{w}}(k) \triangleq \mathbf{w}_o - \mathbf{w}(k)$ and using (7), then (8) is changed as

$$\tilde{\mathbf{w}}(k+1) = [\mathbf{I}_M - \mu \mathbf{A}(k)] \sum_{p=0}^{P-1} \beta_p \tilde{\mathbf{w}}(k-p) - \mu \mathbf{b}(k), \quad (9)$$

where $\mathbf{A}(k) = \mathbf{U}_D(k)\mathbf{A}^{-1}(k)\mathbf{U}_D^T(k)$ and $\mathbf{b}(k) = \mathbf{U}_D(k)\mathbf{A}^{-1}(k)\mathbf{H}^T\boldsymbol{\eta}(k)$. Also, we use the relation $\sum_{p=0}^{P-1}\beta_p = 1$ for deriving (9).

To further continue the analysis, we define some matrices and vectors as follows: $\mathcal{A}(k) = \begin{bmatrix} \mathbf{A}(k) & \mathbf{0}_{M \times M(P-1)} \\ \mathbf{0}_{M(P-1) \times M} & \mathbf{0}_{M(P-1) \times M(P-1)} \end{bmatrix}$,

$$\mathcal{C} = \begin{bmatrix} \boldsymbol{\beta} & \\ \mathbf{I}_{M(P-1)} & \mathbf{0}_{M(P-1) \times M} \end{bmatrix}, \quad \tilde{\mathcal{W}}(k) = \begin{bmatrix} \tilde{\mathbf{w}}(k) \\ \vdots \\ \tilde{\mathbf{w}}(k-P+1) \end{bmatrix}, \quad \mathcal{B}(k) = \begin{bmatrix} \mathbf{b}(k) \\ \mathbf{0}_{M(P-1) \times 1} \end{bmatrix},$$

where $\boldsymbol{\beta} = [\beta_0, \dots, \beta_{P-1}] \otimes \mathbf{I}_M$. Based on these definitions,

(9) can be rewritten in a compact form as

$$\tilde{\mathcal{W}}(k+1) = [\mathbf{I}_{MP} - \mu \mathcal{A}(k)] \mathcal{C} \tilde{\mathcal{W}}(k) - \mu \mathcal{B}(k). \quad (10)$$

For ease of analyses, the following assumptions are necessary.

A1): The system noise $\boldsymbol{\eta}(n)$ is a zero-mean white process with variance σ_η^2 .

A2): $\mathbf{u}(n)$ is zero-mean stationary random vector with positive definite covariance matrix.

A3): $\mathbf{u}_i(k)$ and $\mathbf{w}(k-p)$ for $i=0,1,\dots,N-1$ and $p \leq k$ are statistically independent. This is so-called independence assumption which is commonly used in almost all performance analyses for adaptive algorithms, see [2], [13]-[27].

3.1 Transient-state analysis

Introducing the squared weighted norm of a vector \mathbf{x} , i.e., $\|\mathbf{x}\|_\Sigma^2 = \mathbf{x}^T \Sigma \mathbf{x}$ for any $MP \times MP$ symmetric positive definite matrix Σ , and then applying it into (10), we found the relation

$$\|\tilde{\mathcal{W}}(k+1)\|_\Sigma^2 = \|\tilde{\mathcal{W}}(k)\|_{\mathcal{C}^T [\mathbf{I}_{MP} - \mu \mathcal{A}(k)]^T \Sigma [\mathbf{I}_{MP} - \mu \mathcal{A}(k)] \mathcal{C}}^2 + \mu^2 \mathcal{B}^T(k) \Sigma \mathcal{B}(k) - 2\mu \tilde{\mathcal{W}}^T(k) \mathcal{C}^T [\mathbf{I}_{MP} - \mu \mathcal{A}(k)]^T \Sigma \mathcal{B}(k). \quad (11)$$

From the assumption A3) we can further assume that $\tilde{\mathcal{W}}(k)$ is independent of $\mathcal{A}(k)$ and $\mathcal{B}(k)$. Also, applying the assumption A1), the expectation of the last term of (11) is zero. Consequently, we take the expectation of both sides of (11) as:

$$E\left\{\|\tilde{\mathcal{W}}(k+1)\|_\Sigma^2\right\} = E\left\{\|\tilde{\mathcal{W}}(k)\|_{\Sigma'}^2\right\} + \mu^2 E\left\{\mathcal{B}^T(k) \Sigma \mathcal{B}(k)\right\}, \quad (12)$$

where

$$\Sigma' = E\left\{\mathcal{C}^T [\mathbf{I}_{MP} - \mu \mathcal{A}(k)]^T \Sigma [\mathbf{I}_{MP} - \mu \mathcal{A}(k)] \mathcal{C}\right\}. \quad (13)$$

Aiming to evaluate the moments in (12) and (13), we resort to the vectorization operation and some properties of Kronecker product

[28]. Namely, let $\boldsymbol{\sigma} = \text{vec}(\boldsymbol{\Sigma})$ and $\boldsymbol{\Sigma} = \text{vec}^{-1}(\boldsymbol{\sigma})$. For any matrices $\{\boldsymbol{X}, \boldsymbol{\Sigma}, \boldsymbol{Y}\}$ of compatible dimensions, we have

$$\text{vec}(\boldsymbol{X}\boldsymbol{\Sigma}\boldsymbol{Y}) = (\boldsymbol{Y}^T \otimes \boldsymbol{X}) \text{vec}(\boldsymbol{\Sigma}). \quad (14)$$

Plugging (14) into (13) and using the property $\boldsymbol{X}\boldsymbol{Y} \otimes \boldsymbol{Z}\boldsymbol{\Omega} = (\boldsymbol{X} \otimes \boldsymbol{Z})(\boldsymbol{Y} \otimes \boldsymbol{\Omega})$ for any matrices $\{\boldsymbol{X}, \boldsymbol{Y}, \boldsymbol{Z}, \boldsymbol{\Omega}\}$ of compatible sizes [28], we obtain

$$\boldsymbol{\sigma}' = \text{vec}(\boldsymbol{\Sigma}') = \boldsymbol{F}\boldsymbol{\sigma}, \quad (15)$$

where \boldsymbol{F} is an $M^2 P^2 \times M^2 P^2$ matrix defined by¹

$$\boldsymbol{F} = (\boldsymbol{C} \otimes \boldsymbol{C})^T \left[\boldsymbol{I}_{M^2 P^2} - \mu(\boldsymbol{I}_{MP} \otimes E\{\boldsymbol{A}(k)\}) - \mu(E\{\boldsymbol{A}(k)\} \otimes \boldsymbol{I}_{MP}) + \mu^2 E\{\boldsymbol{A}(k) \otimes \boldsymbol{A}(k)\} \right]. \quad (16)$$

According to the relations $\text{Tr}(\boldsymbol{X}\boldsymbol{Y}) = \text{Tr}(\boldsymbol{Y}\boldsymbol{X})$ and $\text{Tr}(\boldsymbol{X}\boldsymbol{Y}) = (\text{vec}(\boldsymbol{X}^T))^T \text{vec}(\boldsymbol{Y})$ [28], the last term at the right side of (12) can be changed as:

$$E\{\boldsymbol{B}^T(k)\boldsymbol{\Sigma}\boldsymbol{B}(k)\} = E\{\text{Tr}(\boldsymbol{B}(k)\boldsymbol{B}^T(k)\boldsymbol{\Sigma})\} = \text{Tr}(E\{\boldsymbol{B}(k)\boldsymbol{B}^T(k)\boldsymbol{\Sigma}\}) = \text{vec}(E\{\boldsymbol{B}(k)\boldsymbol{B}^T(k)\})^T \boldsymbol{\sigma}. \quad (17)$$

Thus, applying (15)-(17), we rewrite (12) as:

$$E\left\{\left\|\tilde{\boldsymbol{W}}(k+1)\right\|_{\text{vec}^{-1}(\boldsymbol{\sigma})}^2\right\} = E\left\{\left\|\tilde{\boldsymbol{W}}(k)\right\|_{\text{vec}^{-1}(\boldsymbol{F}\boldsymbol{\sigma})}^2\right\} + \mu^2 \boldsymbol{\gamma}^T \boldsymbol{\sigma}. \quad (18)$$

where

$$\boldsymbol{\gamma} = \text{vec}(E\{\boldsymbol{B}(k)\boldsymbol{B}^T(k)\}). \quad (19)$$

Performing repeatedly (18), we have the recursion:

$$E\left\{\left\|\tilde{\boldsymbol{W}}(k+1)\right\|_{\text{vec}^{-1}(\boldsymbol{\sigma})}^2\right\} = E\left\{\left\|\tilde{\boldsymbol{W}}(0)\right\|_{\text{vec}^{-1}(\boldsymbol{F}^{k+1}\boldsymbol{\sigma})}^2\right\} + \mu^2 \boldsymbol{\gamma}^T \sum_{j=0}^{k+1} \boldsymbol{F}^j \boldsymbol{\sigma}, \quad (20)$$

which further yields:

$$E\left\{\left\|\tilde{\boldsymbol{W}}(k+1)\right\|_{\text{vec}^{-1}(\boldsymbol{\sigma})}^2\right\} = E\left\{\left\|\tilde{\boldsymbol{W}}(k)\right\|_{\text{vec}^{-1}(\boldsymbol{\sigma})}^2\right\} - E\left\{\left\|\boldsymbol{W}_o\right\|_{\text{vec}^{-1}(\boldsymbol{F}^{k+1}(\boldsymbol{I}_{M^2 P^2} - \boldsymbol{F})\boldsymbol{\sigma})}^2\right\} + \mu^2 \boldsymbol{\gamma}^T \boldsymbol{F}^{k+1} \boldsymbol{\sigma}. \quad (21)$$

where $\boldsymbol{W}_o = \underbrace{[1, \dots, 1]}_P^T \otimes \boldsymbol{w}_o$, and $\tilde{\boldsymbol{W}}(0) = \boldsymbol{W}_o$ due to the fact that the weight vector is initialized as a null vector.

The MSD is defined as:

$$\text{MSD}(k) \triangleq E\left\{\left\|\tilde{\boldsymbol{w}}(k)\right\|^2\right\}, \quad (22)$$

Therefore, if we choose $\boldsymbol{\Sigma} = \text{diag}(\boldsymbol{\kappa}) \otimes \boldsymbol{I}_M$, i.e., $\boldsymbol{\sigma} = \text{vec}(\text{diag}(\boldsymbol{\kappa}) \otimes \boldsymbol{I}_M)$, then from (21) the MSD evolution of the NR-NSAF algorithm is obtain as:

¹ Here, $\boldsymbol{A}(k) = \boldsymbol{A}^T(k)$ is used.

$$\text{MSD}(k+1) = \text{MSD}(k) - E \left\{ \left\| \mathcal{W}_o \right\|_{\text{vec}^{-1}(\mathbf{F}^k (\mathbf{I}_{M^2 P^2} - \mathbf{F}) \boldsymbol{\sigma})}^2 \right\} + \mu^2 \boldsymbol{\gamma}^T \mathbf{F}^k \boldsymbol{\sigma}, \quad (23)$$

where $\boldsymbol{\kappa}$ is a $P \times 1$ vector whose first element is one and other elements are zero.

To implement (23), some expectations in \mathbf{F} and $\boldsymbol{\gamma}$ are formulated as:

$$E \{ \mathcal{A}(k) \} = \begin{bmatrix} E \{ \mathbf{A}(k) \} & \mathbf{0}_{M \times M(P-1)} \\ \mathbf{0}_{M(P-1) \times M} & \mathbf{0}_{M(P-1) \times M(P-1)} \end{bmatrix}, \quad (24)$$

$$E \{ \mathcal{A}(k) \otimes \mathcal{A}(k) \} = \begin{bmatrix} E \{ \mathbf{A}(k) \otimes \mathbf{A}(k) \} & \mathbf{0}_{M^2 \times M^2(P-1)^2} \\ \mathbf{0}_{M^2(P-1)^2 \times M^2} & \mathbf{0}_{M^2(P-1)^2 \times M^2(P-1)^2} \end{bmatrix}, \quad (25)$$

$$E \{ \mathcal{B}(k) \mathcal{B}^T(k) \} = \begin{bmatrix} E \{ \mathbf{b}(k) \mathbf{b}^T(k) \} & \mathbf{0}_{M \times M(P-1)} \\ \mathbf{0}_{M(P-1) \times M} & \mathbf{0}_{M(P-1) \times M(P-1)} \end{bmatrix}, \quad (26)$$

$$E \{ \mathbf{b}(k) \mathbf{b}^T(k) \} = \sigma_\eta^2 E \{ \mathbf{U}_D(k) \mathbf{A}^{-1}(k) \mathbf{H}^T \mathbf{H} \mathbf{A}^{-1}(k) \mathbf{U}_D^T(k) \}. \quad (27)$$

3.2 Steady-state analysis

According to the assumption A2), it is concluded that $\text{MSD}(k+1) = \text{MSD}(k)$ after the algorithm has reached the steady-state, i.e., $k \rightarrow \infty$. Hence, in the steady-state, (18) reduces to

$$E \left\{ \left\| \tilde{\mathcal{W}}(\infty) \right\|_{\text{vec}^{-1}((\mathbf{I} - \mathbf{F}) \boldsymbol{\sigma})}^2 \right\} = \mu^2 \boldsymbol{\gamma}^T \boldsymbol{\sigma}. \quad (28)$$

By choosing $\boldsymbol{\sigma} = (\mathbf{I} - \mathbf{F})^{-1} \text{vec}(\text{diag}(\boldsymbol{\kappa}) \otimes \mathbf{I}_M)$ in (28), we obtain the steady-state MSD,

$$\text{MSD}(\infty) = \mu^2 \boldsymbol{\gamma}^T (\mathbf{I} - \mathbf{F})^{-1} \text{vec}(\text{diag}(\boldsymbol{\kappa}) \otimes \mathbf{I}_M). \quad (29)$$

3.3 Mean Stability

Under assumptions A1) and A3), the expectation of both sides of (10) is described:

$$E \{ \tilde{\mathcal{W}}(k+1) \} = (\mathbf{I}_{MP} - \mu E \{ \mathcal{A}(k) \}) \mathcal{C} E \{ \tilde{\mathcal{W}}(k) \}. \quad (30)$$

In order to make the convergence of $E \{ \tilde{\mathcal{W}}(k) \}$ as the iteration goes on, the spectral radius of the matrix $\boldsymbol{\Xi} \triangleq [\mathbf{I}_{MP} - \mu E \{ \mathcal{A}(k) \}] \mathcal{C}$ in (30) must be less than 1, i.e., $\rho(\boldsymbol{\Xi}) < 1$. So, we rearrange $\boldsymbol{\Xi}$ as

$$\boldsymbol{\Xi} = \begin{bmatrix} \boldsymbol{\Xi}_0, \boldsymbol{\Xi}_1 & \cdots & \boldsymbol{\Xi}_{P-1} \\ \mathbf{I}_{M(P-1)} & \mathbf{0}_{M(P-1) \times M} & \end{bmatrix}, \quad (31)$$

where $\boldsymbol{\Xi}_p = \beta_p (\mathbf{I}_M - \mu E \{ \mathbf{A}(k) \})$ for $p = 0, 1, \dots, P-1$. Subsequently, we employ the block-maximum-norm of the block matrix defined in [29], with the notation of $\| \cdot \|_{b\infty}$, given as:

$$\begin{aligned}\|\Psi\|_{b_\infty} &\triangleq \max_{\mathbf{x} \neq \mathbf{0}} \left(\frac{\|\Psi\mathbf{x}\|_{b_\infty}}{\|\mathbf{x}\|_{b_\infty}} \right), \\ \|\mathbf{x}\|_{b_\infty} &\triangleq \max_{0 \leq p \leq P-1} \|\mathbf{x}_p\|_2,\end{aligned}\quad (32)$$

where Ψ is an $MP \times MP$ matrix with block entries of size $M \times M$ each, and $\mathbf{x} = [\mathbf{x}_0^T, \dots, \mathbf{x}_{P-1}^T]^T$ an $MP \times 1$ vector with block entries of size $M \times 1$ each. Therefore, we have

$$\|\mathcal{E}\|_{b_\infty} = \max_{\mathbf{x} \neq \mathbf{0}} \frac{\max \left(\sum_{p=0}^{P-1} \|\mathcal{E}_p \mathbf{x}_p\|_2, \|\mathbf{x}_0\|_2, \dots, \|\mathbf{x}_{P-2}\|_2 \right)}{\|\mathbf{x}\|_{b_\infty}} \leq \max_{\mathbf{x} \neq \mathbf{0}} \frac{\max \left(\sum_{p=0}^{P-1} \|\mathcal{E}_p \mathbf{x}_p\|_2, \|\mathbf{x}\|_{b_\infty} \right)}{\|\mathbf{x}\|_{b_\infty}}, \quad (33)$$

$$\sum_{p=0}^{P-1} \|\mathcal{E}_p \mathbf{x}_p\|_2 \leq \|\mathbf{I}_M - \mu E\{\mathcal{A}(k)\}\|_2 \cdot \sum_{p=0}^{P-1} \|\beta_p \mathbf{x}_p\|_2 \leq \|\mathbf{I}_M - \mu E\{\mathcal{A}(k)\}\|_2 \cdot \sum_{p=0}^{P-1} \beta_p \cdot \|\mathbf{x}\|_{b_\infty} = \|\mathbf{I}_M - \mu E\{\mathcal{A}(k)\}\|_2 \cdot \|\mathbf{x}\|_{b_\infty}, \quad (34)$$

thereby yielding

$$\|\mathcal{E}\|_{b_\infty} \leq \max \left(\|\mathbf{I}_M - \mu E\{\mathcal{A}(k)\}\|_2, 1 \right). \quad (35)$$

Because the spectral radius of a matrix is upper bounded by any norm of the matrix [30], we can establish:

$$\rho(\mathcal{E}) \leq \|\mathcal{E}\|_{b_\infty} \leq \max \left(\|\mathbf{I}_M - \mu E\{\mathcal{A}(k)\}\|_2, 1 \right) \leq 1, \quad (36)$$

which leads to the mean convergence condition of the algorithm:

$$\rho(\mathbf{I}_M - \mu E\{\mathcal{A}(k)\}) < 1. \quad (37)$$

By means of the eigenvalue decompositions, (37) simplifies to

$$0 < \mu < \frac{2}{\lambda_{\max}(E\{\mathcal{A}(k)\})}. \quad (38)$$

Note that, (36) also implies that \mathcal{E} could have an eigenvalue λ with $|\lambda| = 1$. However, (37) can remove this possibility. To prove it,

we assume that such an eigenvalue exists, with an $MP \times 1$ eigenvalue vector \mathbf{x} consisting of $\mathbf{x} = [\mathbf{x}_0^T, \dots, \mathbf{x}_{P-1}^T]^T$, where \mathbf{x}_p is an

$M \times 1$ vector for each p . Also, again using (31), we have the following relation :

$$\begin{aligned}\mathcal{E}\mathbf{x} = e^{j\theta} \mathbf{x} \Rightarrow \\ \left[\sum_{p=0}^{P-1} (\mathcal{E}_p \mathbf{x}_p)^T, \mathbf{x}_0^T, \dots, \mathbf{x}_{P-2}^T \right]^T = e^{j\theta} \left[\mathbf{x}_0^T, \dots, \mathbf{x}_{P-1}^T \right]^T,\end{aligned}\quad (39)$$

which further reduces to:

$$\left[\sum_{p=0}^{P-1} \mathcal{E}_p e^{-j(p+1)\theta} \right] \mathbf{x}_{P-1} = \mathbf{x}_{P-1}, \quad (40)$$

where θ is an angle. By the triangular inequality of norms, we obtain:

$$\left\| \sum_{p=0}^{P-1} \mathcal{E}_p e^{-j(p+1)\theta} \right\|_2 \leq \sum_{p=0}^{P-1} \|\mathcal{E}_p e^{-j(p+1)\theta}\|_2 \leq \sum_{p=0}^{P-1} \|\mathcal{E}_p\|_2 = \left(\sum_{p=0}^{P-1} \beta_p \right) \|\mathbf{I}_M - \mu E\{\mathcal{A}(k)\}\|_2 < 1, \quad (41)$$

Since (41) is contradiction to the assumption of $|\lambda|=1$, the proof is completed.

4. Simulation results

Simulations are presented to evaluate the theoretical results of the NR-NSAF algorithm. Both the adaptive filter and unknown system have the same length of $M=16$. The correlated input signal $u(n)$ is generated by filtering either a white Gaussian process with zero mean and unit variance or a uniform distribution process over the interval $[-1, 1]$, through a first-order autoregressive system with a pole at 0.9 [21], called as the Gaussian input and the uniform input, respectively. The system noise $\eta(n)$ is a zero mean white Gaussian process, giving to a certain signal-to-noise rate (SNR). The cosine modulated filter banks are used for the subband structure; the length of the prototype filter is 32 and 64 for the number of subbands $N=4$ and 8, respectively. The expectation values in (24)-(27) are estimated by ensemble averaging. The regularization constant ε is set to 0.001, except for Fig. 8. The simulations results are averaging over 200 trials.

4.1 Transient results

To begin with, we check the mean convergence behavior of the algorithm in Fig. 2. The unknown vector is $\mathbf{w}_o=[0.51, -0.04, 0.02, 0.09, 0.22, 0.20, 0.13, -0.48, -0.39, 0.32, -0.11, -0.30, 0.25, -0.24, 0.6, -0.01]^T$. As shown in Fig. 2, the theoretical mean of weights given by (30) agrees with the simulation results well.

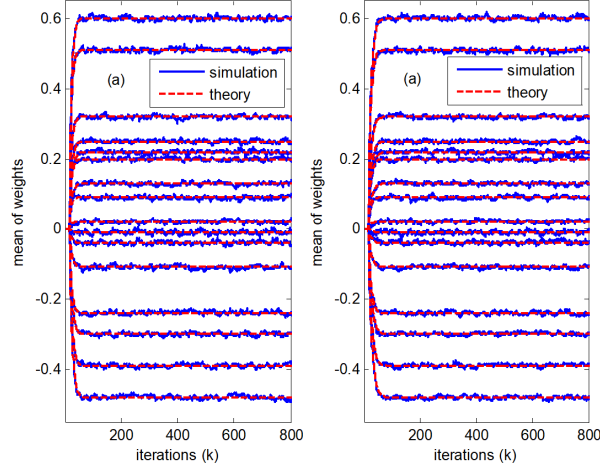


Fig. 2 Mean convergence behavior of the NR-NSAF algorithm. (a) $\alpha = 0.5$, (b) $\alpha = 1$. [Gaussian input, SNR=10 dB, $\mu=0.4$, $N=8$ and $P=3$].

Then, in the following examples of mean square behavior, the unknown vector is randomly generated by using the $rand(M, 1) - 0.5$ function in MATLAB, and normalized to have a unit Euclidean norm. The MSD, $10 \log_{10} [\text{MSD}(k)]$ (dB), is used to plot these results.

Fig. 3 shows the effect of the parameter α on the MSD performance of the NR-NSAF algorithm. The theoretical MSD curves are obtained by performing (23). As can be seen, the theory values have good agreement with simulations. Also, the value of α is closer to 1, the steady-state MSD is lower while retaining comparable convergence. So, $\alpha = 1$ is preferred for this algorithm, also due to the

increased computational amount for $\alpha \neq 1$.

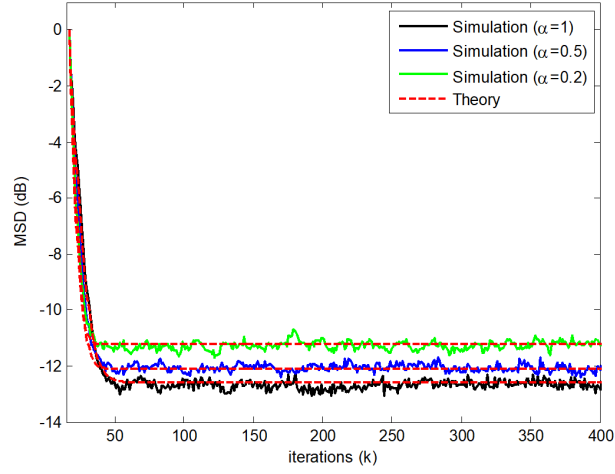


Fig. 3 MSD curves of the NR-NSAF algorithm using different α values. [Gaussian input, SNR = 10 dB, $\mu = 0.4$, $N = 8$ and $P = 3$].

Fig. 4 plots the MSD curves of the NR-NSAF algorithm (with $P=1, 2, 3$ and 4 values), where the NR-NSAF equals to the NSAF when $P=1$. It is clear to see that the theory curves can match well with the simulated curves. From Fig. 4(a), we find that the steady-state MSD of the NR-NSAF algorithm gets lower as P increases in low SNR cases, while maintaining comparable convergence rate. On the other hand, as one can see in Fig. 4(b), the convergence rate also slows with the increasing of P in high SNR cases. It follows that the NR-NSAF algorithm is suitable for highly noisy scenario.

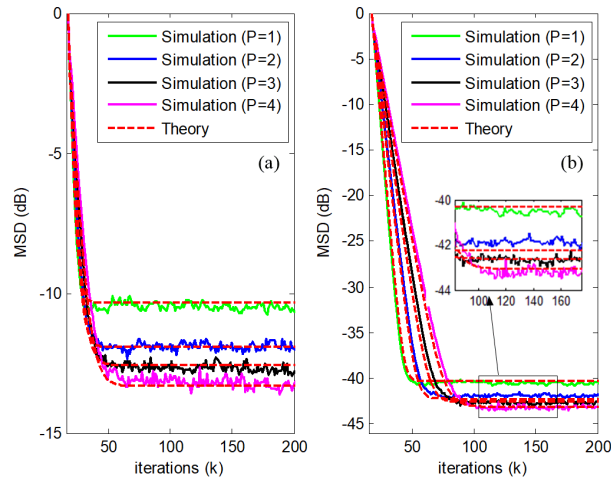
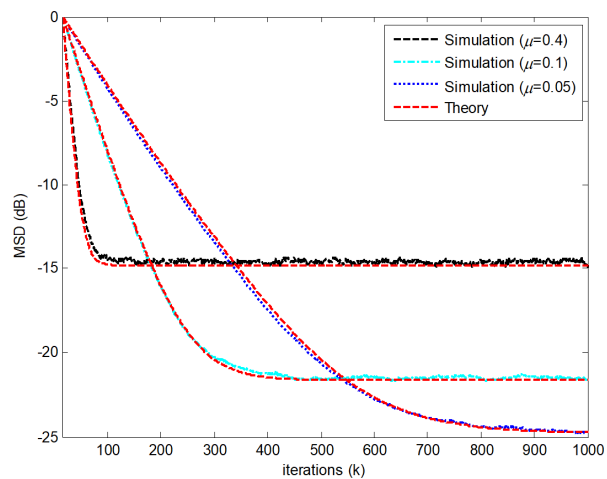
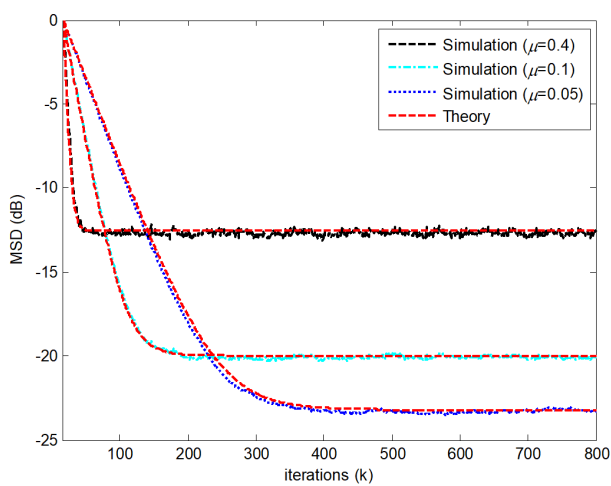


Fig. 4 MSD curves of the NR-NSAF algorithm versus different values of P . (a) SNR=10 dB, (b) SNR=40 dB. [$\mu = 0.4$, $N = 8$, and $\alpha = 1$].

In Figs. 5 and 6, the MSD performance curves of the NR-NSAF using different step sizes ($\mu = 0.05, 0.1$ and 0.4) are shown for the Gaussian input and the uniform input, respectively. As one can see, the theoretical results are very close to the simulated results. Moreover, the NR-NSAF algorithm has a compromise between the convergence rate and steady-state MSD on choosing the step size.

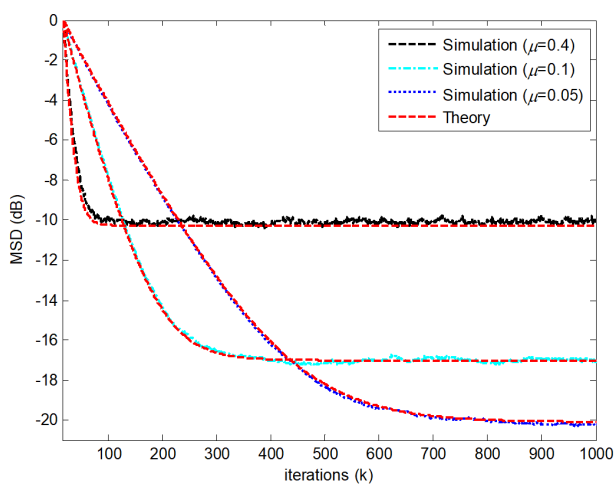


(a)

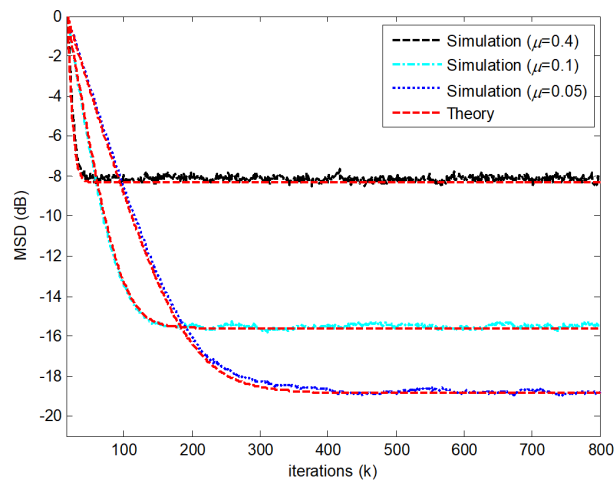


(b)

Fig. 5 MSD curves of the NR-NSAF algorithm versus different step sizes for Gaussian input. (a) $N = 4$, (b) $N = 8$. [SNR = 10 dB, $P = 3$, and $\alpha = 1$].



(a)

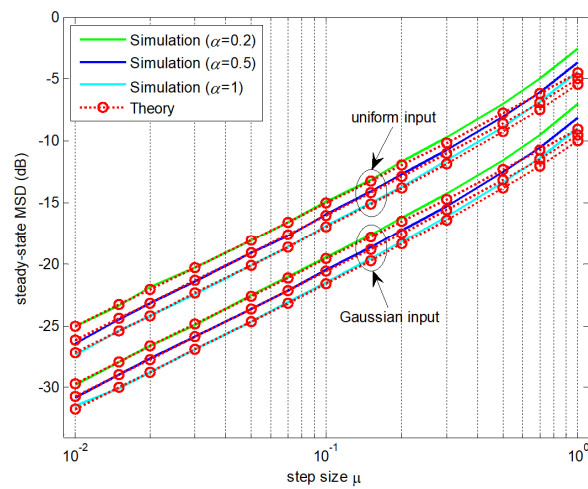


(b)

Fig. 6 MSD curves of the NR-NSAF algorithm versus different step sizes for uniform input. (a) $N = 4$, (b) $N = 8$. [SNR = 10 dB, $P = 3$, and $\alpha = 1$].

4.2 Steady-state results

In this subsection, we examine the steady-state MSD of the NR-NSAF algorithm as a function of the step size. The simulation values are obtained by averaging more than 500 instantaneous MSD values in the steady-state, and the theory values are computed according to (29). The step size μ varies from 0.01 to 1.0.



(a)

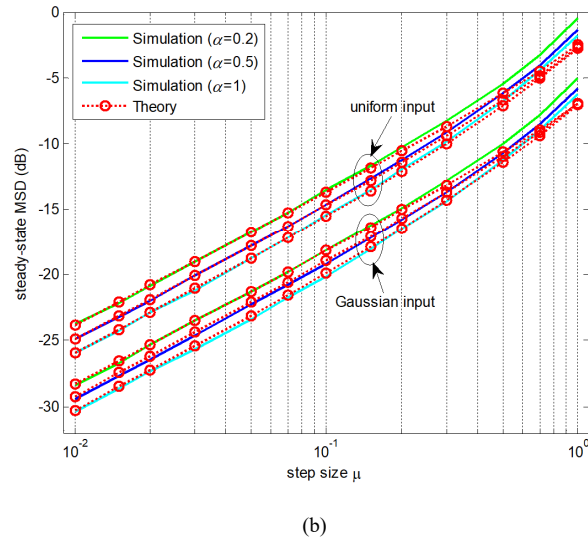
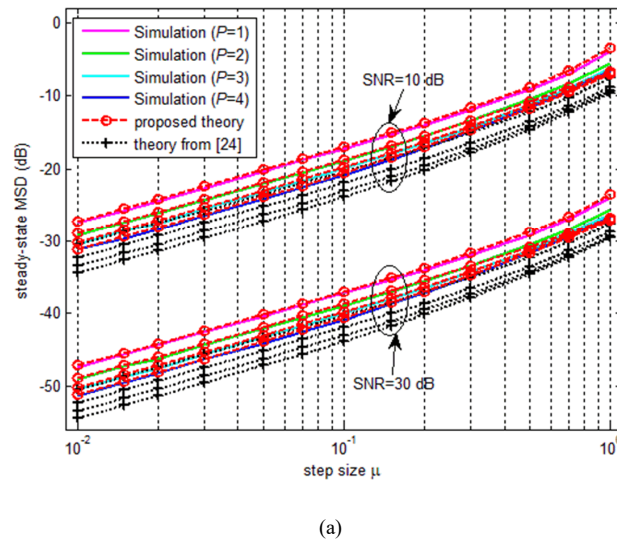


Fig. 7 Steady-state MSDs of the NR-NSAF algorithm with different α values. (a) $N=4$, (b) $N=8$. [SNR=10 dB and $P=3$].

Fig. 7 shows the steady-state MSD results of the NR-NSAF algorithm using $\alpha=0.2, 0.5$ and 1 values, where the other setting is the same as Fig. 3. We can observe from this figure a good agreement between the theoretical values and simulated values for small step sizes. Next, to fairly comparing the proposed (38) with the theoretical model in [24], we consider a special form of the NR-NSAF algorithm in Fig. 8. Namely, the value of α is set to 1 and the regularization constant ε is set to 0 . As can be seen from Fig. 8, the proposed theoretical results have a good match with the simulated results when the step size is small. However, a discrepancy of them can also be observed in Figs. 7 and 8 for large step sizes. This is due mainly to the fact that the independence assumption A3) used in the analysis is valid in general for a small step size [2]. In comparison, the proposed theory (38) works better than the theory from [24] used for predicting the steady-state MSD of the NR-NSAF algorithm. This is because that the theory model in [24] relies on two additional assumptions that the subband input signals are white (requiring large enough number of subbands), and the adaptive filter is long.



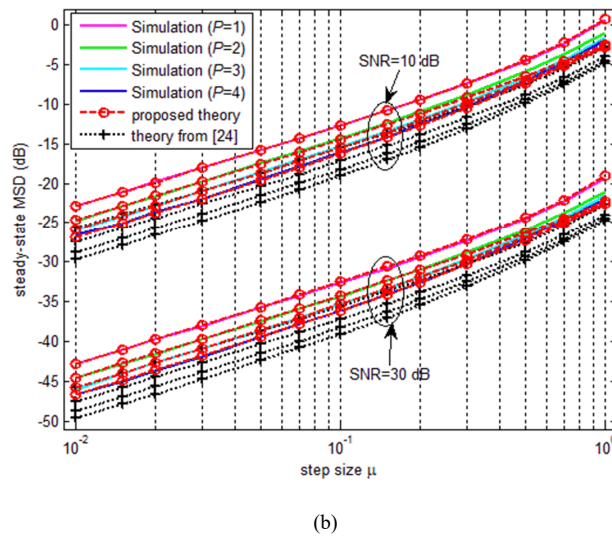


Fig. 8 Steady-state MSD curves of the NR-NSAF algorithm. (a) Gaussian input, (b) uniform input. [$N=8$].

5. Conclusion

In this study, we have presented a very detailed performance analysis for the NR-NSAF algorithm in terms of the transient-state and steady-state MSD. The proposed analysis is based on the method of the vectorization operation and the Kronecker product so that it does not restrict the distribution of the input signal. In addition, the paraunitary assumption imposed on the analysis filter banks is not necessary in our analysis. For the simplified INSAF algorithm, the proposed steady-state expression outperforms the previous theory in [24] for a low-order adaptive filter. Simulation results in various environments have shown good agreement with the theoretical results.

Acknowledgement

This work was partially supported by National Science Foundation of P.R. China (Grant: 61271340, 61571374 and 61433011).

References

- [1] J. Benesty, and Y. Huang, Adaptive signal processing—applications to real-world problems, Berlin, Germany: Springer-Verlag, 2003.
- [2] A. H. Sayed, Fundamentals of Adaptive Filtering. Hoboken, NJ, USA: Wiley, 2003.
- [3] K. A. Lee, and W. S. Gan, “Improving convergence of the NLMS algorithm using constrained subband updates,” IEEE Signal Process. Lett., vol. 11, no. 9, pp. 736–739, 2004.
- [4] J. Ni, and F. Li, “A variable step-size matrix normalized subband adaptive filter,” IEEE Trans. Audio Speech Lang. Process., vol. 18, no. 6, pp. 1290–1299, 2010.
- [5] J. J. Jeong, K. Koo, G. T. Choi, and S. W. Kim, “A variable step size for normalized subband adaptive filters,” IEEE Signal Process. Lett. vol. 19, no. 12, pp. 906–909, 2012.
- [6] J. H. Seo, and P. G. Park, “Variable individual step-size subband adaptive filtering algorithm,” Electron. Lett., vol. 50, no. 3, pp. 177–178, 2014.
- [7] F. Yang, M. Wu, P. Ji, and J. Yang, “An improved multiband-structured subband adaptive filter algorithm,” IEEE Signal Process. Lett., vol. 19, no. 10, pp. 647–650, 2012.
- [8] Y. S. Choi, S. E. Kim and W.J. Song, “Noise-robust normalised subband adaptive filtering,” Electronics Letters, vol. 48, no. 8, 432–434, 2012.
- [9] J. Ni, “Improved normalised subband adaptive filter,” Electron. Lett., vol. 48, no. 6, pp. 320–321, 2012.

- [10] H. Zhao, Z. Zheng, Z. Wang, B. Chen, "Improved affine projection subband adaptive filter for high background noise environments," *Signal Processing*, 137: 356-362, 2017.
- [11] Y. Yu, H. Zhao, B. Chen, "Set-membership improved normalised subband adaptive filter algorithms for acoustic echo cancellation," *IET Signal Processing*, vol. 12, no. 1, pp. 42–50, 2018.
- [12] H. Cho, C. W. Lee, S. W. Kim, "Derivation of a new normalized least mean squares algorithm with modified minimization criterion," *Signal Processing*, vol. 89, no. 4, pp. 692–695, 2009.
- [13] H. C. Shin, A.H. Sayed, "Mean-square performance of a family of affine projection algorithms," *IEEE Trans. Signal Process.*, vol. 52, no. 1, pp. 90–102, 2004.
- [14] S. Zhang, J. Zhang, H. C. So, "Mean square deviation analysis of LMS and NLMS algorithms with white reference inputs," *Signal Processing*, vol. 131, pp. 20-26, 2017.
- [15] S. E. Kim, J. W. Lee, W. J. Song, "A theory on the convergence behavior of the affine projection algorithm," *IEEE Trans. Signal Process.*, vol. 59, no. 12, pp. 6233–6239, 2011.
- [16] S. E. Kim, J. W. Lee, and W. J. Song, "A noise-resilient affine projection algorithm and its convergence analysis," *Signal Process.*, vol. 121, pp. 94–101, 2016.
- [17] M. S. E. Abadi, M. S. Shafiee, M. Zalahi. "A low computational complexity normalized subband adaptive filter algorithm employing signed regressor of input signal," *EURASIP Journal on Advances in Signal Processing*, vol. 2018, no. 1, pp. 1–23, 2018.
- [18] K. A. Lee, W. S. Gan, and S. M. Kuo, "Mean-square performance analysis of the normalized subband adaptive filter," in *Proc. 40th Asilomar Conf. Signals, Syst., Comput.*, 2006, pp. 248–252.
- [19] J. Ni and X. Chen, "Steady-state mean-square error analysis of regularized normalized subband adaptive filters," *Signal Process.*, vol. 93, no. 9, pp. 2648–2652, 2013.
- [20] W. Yin, and A. S. Mehr, "Stochastic analysis of the normalized subband adaptive filter algorithm," *IEEE Trans. Circuits Syst. I: Reg. Pap.*, vol. 58, no. 5, pp. 1020–1033, 2011.
- [21] J. J. Jeong, S. H. Kim, G. Koo, and S. W. Kim, "Mean-square deviation analysis of multiband-structured subband adaptive filter algorithm," *IEEE Trans. Signal Process.* vol. 64, no. 4, pp. 985–994, 2016.
- [22] Y. Yu and H. Zhao, "Performance analysis of the deficient length NSAF algorithm and a variable step size method for improving its performance," *Digital Signal Processing*, vol. 62, pp. 157-167, 2017.
- [23] F. Yang, M. Wu, P. Ji, Z. Kuang, and J. Yang, "Transient and steady-state analyses of the improved multiband-structured subband adaptive filter algorithm," *IET Signal Process.*, vol. 9, no. 8, pp. 596–604, 2015.
- [24] J. J. Jeong, K. Koo, G. Koo, and S. W. Kim, "Steady-state mean-square deviation analysis of improved normalized subband adaptive filter," *Signal Process.*, vol. 106, pp. 49–54, 2015.
- [25] Y. Yu, H. Zhao, and L. Lu, "Steady-state behavior of the improved normalized subband adaptive filter algorithm and its improvement in under-modeling," *Signal, Image and Video Processing*, vol. 12, no. 4, pp. 617–624, 2018.
- [26] T. Y. Al-Naffouri and A. H. Sayed, "Transient analysis of adaptive filters with error nonlinearities," *IEEE Trans. Signal Process.*, vol. 51, no. 3, pp. 653-663, 2003.
- [27] B. Chen, L. Xing, H. Zhao, N. Zheng, J.C. Principe, "Generalized correntropy for robust adaptive filtering," *IEEE Trans. Signal Process.*, vol. 64, no. 13, pp. 3376–3387, 2016.
- [28] G. Alexander, *Kronecker products and matrix calculus with applications*. New York: Halsted, 1981.
- [29] A. H. Sayed, "Diffusion adaptation over networks," *E-Reference Signal Processing*, S. Theodoridis and R. Chellapa, Eds. Amsterdam, The Netherlands: Elsevier, 2013.
- [30] R. A. Horn, C. R. Johnson, *Matrix analysis*, Cambridge university press, 2012.